TWENTYFITH EUROPEAN ROTORCRAFT FORUM

Paper n° B9

DIRECT BVI–SOUND PRESSURE CALCULATION BY USING AERODYNAMIC DATA AND APPLICATION OF RETARDED POTENTIALS

BY

L. ZERLE, S. WAGNER

UNIVERSITÄT STUTTGART
INSTITUT FÜR AERODYNAMIK UND GASDYNAMIK
STUTTGART, GERMANY

SEPTEMBER 14–16, 1999
ROME
ITALY

ASSOCIAZIONE INDUSTRIE PER L'AEROSPAZIO, I SISTEMI E LA DIFESA
ASSOCIAZIONE ITALIANA DI AERONAUTICA ED ASTRONAUTICA

DIRECT BVI–SOUND PRESSURE CALCULATION BY USING AERODYNAMIC DATA AND APPLICATION OF RETARDED POTENTIALS

L. ZERLE and S. WAGNER
Institut für Aerodynamik und Gasdynamik
Universität Stuttgart
Pfaffenwaldring 21, D–70550 Stuttgart
Federal Republic of Germany

ABSTRACT

Together with the basis of a time–stepping aerodynamic free wake rotor code, 'retarded potentials' allow the calculation of BVI sound pressure generated by the rotor. This is caused by a strong link between aerodynamics and aeroacoustics within the boundary element methods (BEM). The aerodynamic computer code is an extended panel method which develops the free moving rotor wake lattice time–stepwise. It is able to deal with strong blade–vortex interaction (BVI) and arbitrary rotorblade motion in every flight condition. The timestep method allows the storage of the whole space–time moving history of blades and wakes. This enables us to regard the limited propagation speed of information in the flow field, which concerns beside pressure signals all singularity activities on the panel surface. This is based on the wave equation, formulated in the 'airframe of reference' coordinate system. The induced potential values, radiated from the singularities at the retarded panel positions, are determined and directly used for BVI sound pressure derivation at every timestep. There is no necessity to calculate the sound pressure via blade surface pressure evaluation. Graphical visualization of the retarded rotor position in relation to the rotorblade wake (tip vortex) position at timesteps of interest is possible and provides deep technical insight. A further benefit of this BVI mechanism investigation is the ability of 'influence decomposition', i.e. the contribution of different blades or blade sections can be calculated by the postprocesor seperately. In the present paper the applied retarded potential method is explained in detail and first comparisons with measurements are included.

1. Introduction

One of the most important fields of current rotorcraft research includes methods for noise reduction. To achieve progress in this field it is necessary to use modern computer methods to predict sound pressure with sufficient accuracy. The enlargement and refinement of the background knowledge about the very complex flow behaviour around a helicopter rotor is the basis for further improvements and the application of new concepts such as individual blade control (IBC). Rotor noise itself is generated by different types of sources and one of them is the so–called 'blade–vortex interaction' (BVI), where the rotorblades hit their own trailing vortices. Especially the descent flight path is affected by BVI and its noise emission.

To model the aerodynamic rotor wake system different methods were developed. One of them is the 'Free Wake Vortex Lattice' method, based on an extended panel method and potential theory. Compared to other methods, this panel method is a very fast method and requires only limited modern computer resources. This aerodynamic method also guarantees a good representation of rotorwake activity towards the rotorblades and gives a good illustration of vortex core positions within the rotor flow field. Beside lift and flowfield calculations the free wake vortex lattice method was already used to supply start and boundary conditions for a rotor flow calculation by EULER method [16], resulting in a significant computer time reduction.

For several years the author has investigated a new application of the free wake vortex lattice method, following some ideas of a fundamental linkage between aerodynamics and acoustics.

The method of 'Retarded Potentials' accounts for the limited speed of information propagation and also limited propagation of singularity activity within the flow field. A limited propagation speed of singularity activity within flow calculation was theoretically introduced by PRANDTL [12] already in 1936, where an acceleration potential was adressed. The wave equation for small disturbances given there is also a fundamental equation in acoustics. In the acoustic domain the fundamentals and mathematical derivations of FFOWCS WILLIAMS and HAWKINGS [5] and FARASSAT [3, 4] are referenced. There the sound pressure in the flow field is calculated by evaluation of the unsteady pressure behavior at the rotorblade surfaces. Another approach, especially for BVI noise, is given by [9], where the local BVI incidence at the blade is regarded as a sound source which is moving spanwise along the blade. Important relations between aerodynamics and acoustics were developed within a large number of publications by MORINO [10, 6]. To deal with the time–retarded influence of flow field singularities such as blade panels, the kinematics and functions of influence of the moving singularities are essential. The work of DAS [2, 1] develops the analytical handling of translatoric and helical moving singularities.

The goal of the current work is the evaluation of the aerodynamic rotorblade and wake data by a 'retarded potential' postprocessor code to calculate the BVI sound pressure at arbitrary observer points. Important aspects are 1) the determination of the retarded blade and wake geometry of the fully articulated rotor, 2) the evaluation of the induced potential which is radiated by the moving panels and 3) the ability of influence decomposition to locate the areas of BVI sound emission. All investigations as presented here were done with an isolated rotor. No fuselage was included.

Extensive, aerodynamic and acoustic windtunnel data were collected within the research program of the European Union (IMT–HELISHAPE) [15], where the Institute was involved as a partner. Measurements from there are used for comparisons.

2. Aerodynamic Code

The applied aerodynamic code, the 'Rotor Free Wake Vortex Lattice Method' (ROVLM) was developed at the institute during several years. Some features are only very briefly described here, without giving any formulas. The method is an extended, inhouse developed panel code following linear velocity potential theory and working in a time–stepping manner. The doublet strength of the new built spanwise wake row at the end of each timestep is obtained from the blade trailing edge panels at every spanwise section. Basics of this method together with a lot of extensions and applications have been already published [13, 17, 18, 14]. In the current version, the code is working with a thick paneled rotorblade model and applies the internal Dirichlet Boundary condition for the potential at the control points of each blade panel. For profound and detailed information about panel method basics and applications the reader is referred to [7]. Important features of the code are:

- The code runs stable in each flight condition. Even local blade penetration by wake–vortex filaments does not affect the code run or the results in a negative way. Of special interest are situations with direct contact of blade and wake lattice, the so–called strong BVI. This is important in descent forward flight conditions with severe BVI activity. Such a typical situation is presented in Figure 1, where the rotor is partially hidden by the wake lattice.

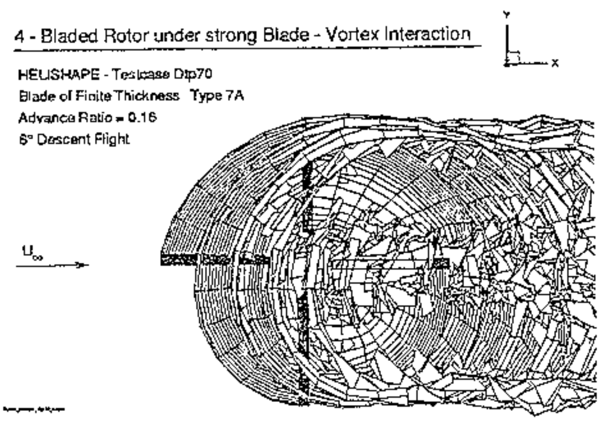

Figure 1: Calculated vortex lattice system of a HELISHAPE testcase

- A practicable model to deal with reverse flow at the inner rotorblade airfoil sections in forward flight is included.
- Calculated source and doublet strength of each blade panel and the corresponding geometrical blade network data are to be stored in a datafile to remain accessible for the 'retarded potential' postprocessor.
- A variable timestep length strategy is selected. The start–up wake is calculated with 15° rotorangle timesteps until cyclic steady state conditions are achieved. After an intermediate phase of 5° timesteps, a decrease to 1° timestep length is done, especially for those timesteps which will be allocated by the postprocessor to perform sound pressure calculation.
- All rotor blade movements such as rotation, collective pitch, cyclic pitch and blade flapping are code input parameters.

3. The Mathematical Background of 'Retarded Potenials'

Starting with the full potential equation

$$\left(1-\frac{u^2}{a^2}\right)\frac{\partial^2\Phi}{\partial x^2}+\left(1-\frac{v^2}{a^2}\right)\frac{\partial^2\Phi}{\partial y^2}+ + \left(1-\frac{w^2}{a^2}\right)\frac{\partial^2\Phi}{\partial z^2} - -\frac{2uv}{a^2}\frac{\partial^2\Phi}{\partial x\partial y}-\frac{2vw}{a^2}\frac{\partial^2\Phi}{\partial y\partial z}-\frac{2wu}{a^2}\frac{\partial^2\Phi}{\partial z\partial x}- -\frac{2u}{a^2}\frac{\partial^2\Phi}{\partial x\partial t}-\frac{2v}{a^2}\frac{\partial^2\Phi}{\partial y\partial t}-\frac{2w}{a^2}\frac{\partial^2\Phi}{\partial z\partial t}- -\frac{1}{a^2}\frac{\partial^2\Phi}{\partial t^2}=0 \quad (1)$$

and two important assumptions:

- Formulations and calculations are done within a non moving coordinate system which is called the 'Airframe of Reference'
- Speed of sound $a = a_0$ is regarded to be constant, which is a good approximation in subsonic condition up to $Ma = 0,7$.

we obtain the wave equation for the velocity potential:

$$\nabla^2\Phi - \frac{1}{a_0^2}\cdot\frac{\partial^2\Phi}{\partial t^2} = 0 \quad (2)$$

The solution of this wave equation can be traced back to KIRCHHOFF 1883 [8, 3]. An extended GREEN function (3) is used. It includes the DIRAC function which performs a kind of filtering with respect to the limited speed of pressure wave and singularity activity propagation:

$$G = \frac{1}{r_{ret}}\cdot\delta(t-t_e+\frac{r_{ret}}{a_0}) \quad (3)$$

Inserting this formula into:

$$\Phi_P = \frac{1}{4\pi}\iint_S -\frac{\partial\Phi}{\partial n}G\,d\mathcal{S} + \frac{1}{4\pi}\iint_S \Phi\frac{\partial G}{\partial n}d\mathcal{S} \quad (4)$$

one yields the solution of the wave equation [11, 4]:

$$\begin{aligned}\Phi_P &= \frac{1}{4\pi}\iint_S -\frac{\partial\Phi}{\partial n}\frac{1}{r_{ret}}d\mathcal{S} + \\ &+ \frac{1}{4\pi}\iint_S \Phi\cdot\frac{\vec{e}_\mu\cdot\vec{r}_{ret}}{r_{ret}^3}d\mathcal{S} + \\ &+ \frac{1}{4\pi}\iint_S \frac{\dot{\Phi}}{a_0}\cdot\frac{\vec{e}_\mu\cdot\vec{r}_{ret}}{r_{ret}^2}d\mathcal{S} \quad (5)\end{aligned}$$

Including now the elements of classical panel methods such as sources and doublets at blade and wake surfaces we get an equation for the potential value Φ_P in the flow field, related to Figure 2:

$$\begin{aligned}\Phi_P &= \underbrace{\frac{1}{4\pi}\iint_S -\sigma\cdot\frac{1}{r_{ret}}d\mathcal{S}}_{Source} + \quad (6)\\ &+ \underbrace{\frac{1}{4\pi}\iint_S \mu\cdot\frac{\vec{e}_\mu\cdot\vec{r}_{ret}}{r_{ret}^3}d\mathcal{S}}_{Doublet} + \\ &+ \underbrace{\frac{1}{4\pi}\iint_S \frac{\dot{\mu}}{a_0}\cdot\frac{\vec{e}_\mu\cdot\vec{r}_{ret}}{r_{ret}^2}d\mathcal{S}}_{Ratelet} + \\ &+ \underbrace{\frac{1}{4\pi}\iint_W \mu_W\cdot\frac{\vec{n}\cdot\vec{r}_{ret}}{r_{ret}^3}d\mathcal{W}}_{Wake-Doublet}\end{aligned}$$

Some explanations about the formula elements:

1) $\vec{r}_{ret}$ represents the vector from the sending location of the singularity, i.e. retarded position of the source or doublet panel, to the observer

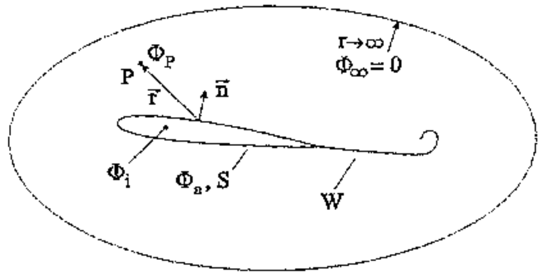

Figure 2: Velocity Potential in the Flowfield

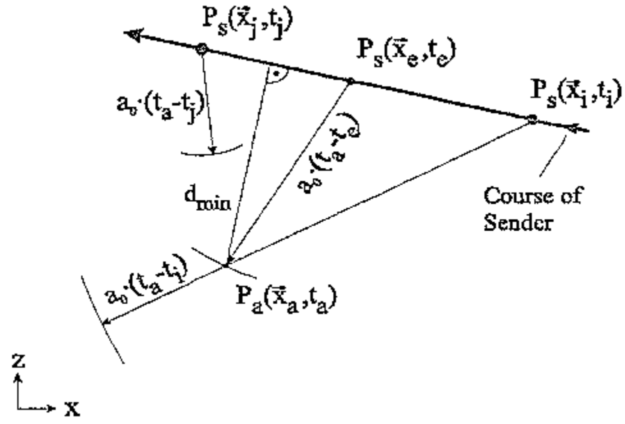

Figure 3: Determination of the sending position, indicated by 'e'

P
2) $\vec{e}_\mu$ is the doublet direction unit vector of the panel in retarded position, which may be no longer perpendicular towards the panel surface.
3) The part in the equation underbraced by 'Ratelet' arises during the difficult differentiation of the DIRAC function in formula (3) and (4) by chain rule. It is not a new kind of singularity, but the time derivative of the panel doublet strength is the governing value here. Influence decrease with respect to distance goes only by $1/r$ which is important for the far field. In the calculations presented later it was detected that the 'Ratelet' dominates the BVI originated sound pressure.
4) Compared with the rotorblades, the wake doublet strength remains constant i.e. there is no wake–ratelet activity. In view of the relatively low wake speed in the airframe of reference, the doublet vector $\vec{n}$ is assumed to remain perpendicular.

4. Calculation of the Retarded Position

The retarded position of moving singularities is the key of the whole method. Following Figure 3, the correct sending positions $\vec{x}_e$ at time t_e of the moving singularity P_s towards an observer P_a with given observing time t_a is determined by the investigation of the space–time moving history of the singularity. It is regarded as a sender. The arbitrary movement is already discreticed by the time–stepping, aerodynamic free wake code and stored by the space–time points $P_S(\vec{x}_i, t_i)$. A simple example of a straight translatoric movement between the space–time points i and j is illustrated in Figure 3.

Our desired sending position is $P_s(\vec{x}_e, t_e)$, which is now determined on the assumption of translatoric movement and constant speed between the positions i and j. A modified MINKOWSKI–Diagram (Fig. 4) illustrates this situation, where the function of the distance d between the points P_s and P_a versus time is given. With the restriction $t < t_a$ the distance function is:

$$d(t) = |\vec{x}(t) - \vec{x}_a(t_a)| \tag{7}$$

and the condition for transmission time and distance obeys the equation

$$a_0 \cdot (t_a - t_e) = |\vec{x}(t_e) - \vec{x}_a(t_a)| \tag{8}$$

Using the known points $P_S(\vec{x}_i, t_i)$ and $P_S(\vec{x}_j, t_j)$ and assuming a constant, linear movement of the sender P_S, we obtain the linear, local equation of movement:

$$\vec{x}(t) = \frac{\vec{x}_j - \vec{x}_i}{t_j - t_i} \cdot t + \vec{x}_i \tag{9}$$

which is inserted with $t = t_e$ into (8). Now we receive a quadratic equation to calculate

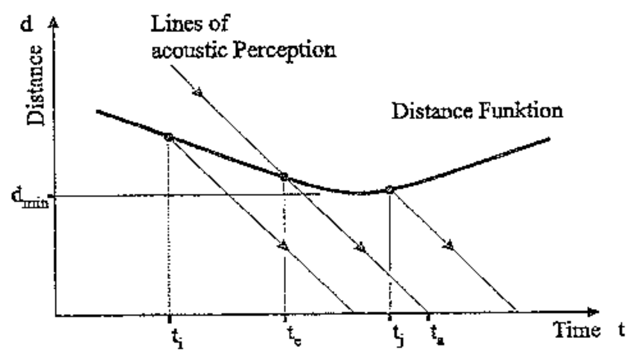

Figure 4: Modified MINKOWSKI–Diagram, Distance $d(P_a, P_s)$ versus Time

t_e and together with (9) the exact location of emission $\vec{x}(t_e)$ is determined. Starting with the 'youngest' available position of the P_S moving history, the method developed here leads directly to the retarded position, without any iteration.

The retarded position of a whole rotorblade is determined by application of the described method at every panel nodal point as given in Figure 5 where the shape of earlier rotorblade positions is indicated, too. The observer P_a receives at t_a the induction of all the singularity activities at the retarded rotorblade. It is like to see the rotorblade 'acoustically'.

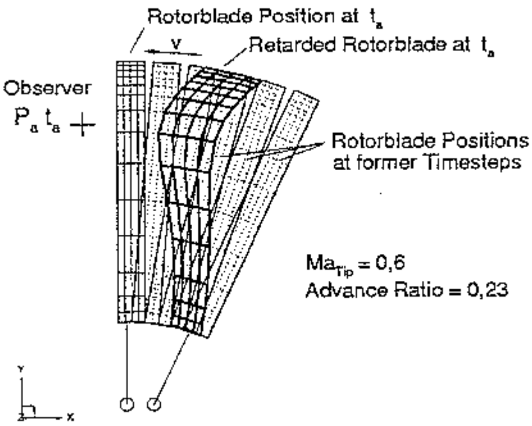

Figure 5: Retarded rotorblade, together with blade positions at current and earlier timesteps

Seeing the completely retarded rotor in Figure 6 we detect that the retarded panels have different size, approaching panels appear to be enlarged, leaving panels seem to be reduced. This links up to the next chapter.

5. Singularity Activity in Retarded Position

To evaluate the induction of moving singularities, the following effects are taken into account:

1) Sending (retarded) position and real position are different.

2) The 'volume of emissions' changes, already visible by a different panel size. But that is only one part. If we look for example at a 3-dimensional spatial distributed source there is also a change in panel thickness from ds_0 to ds_ν, as it is demonstrated in Figure 7. In

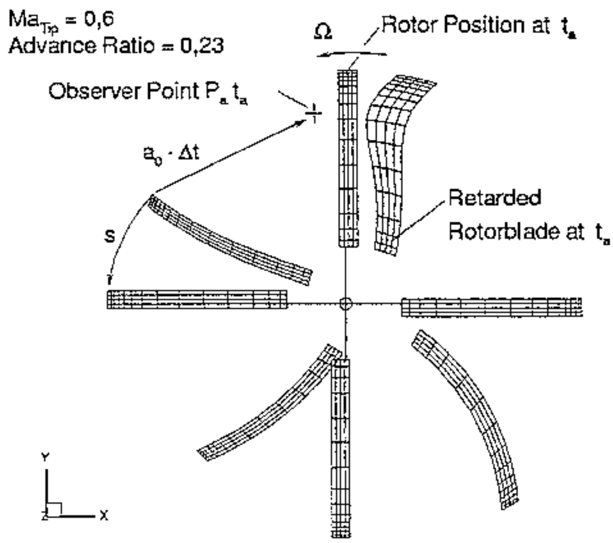

Figure 6: Retarded rotor position

this special case the panel moves with subsonic MACH-number Ma_S parallel to the x–axis. The model of the infinite thin panel has been extendend by a volume factor which accounts for the change of thickness if the panel influence is evaluated in retarded position. Changes in panel aera size like dl_0 to dl_ν are already represented by the retarded position of the panel edge points.

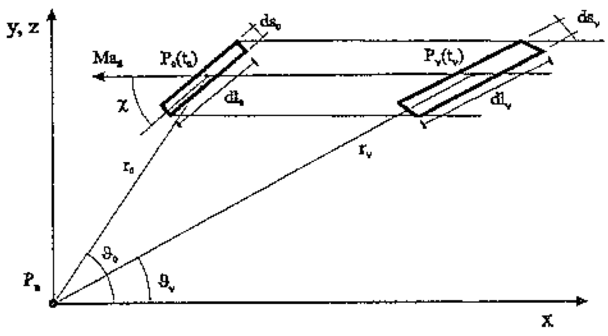

Figure 7: Variation of panel thickness ds_0 and panel length dl_0. Index ν indicates retarded positions

3) Now we consider a doublet panel which is orginally built by a pair of source and sink with distance ds_μ as it is shown in Figure 8. There is a tilt angle χ_ν which remains unchanged, even in the case of infinitesimal distance $ds_\mu \to 0$. Therefore a change of induced doublet activity occurs. The doublet direction vector in re-

tarded position is $\vec{e}_\mu$ instead of $\vec{n}$.
In the current retarded potential code the effects 2) and 3) are accounted for by additional geometrical points in the direct vicinity of the panel. They are treated by the same procedure as the panel edge points.

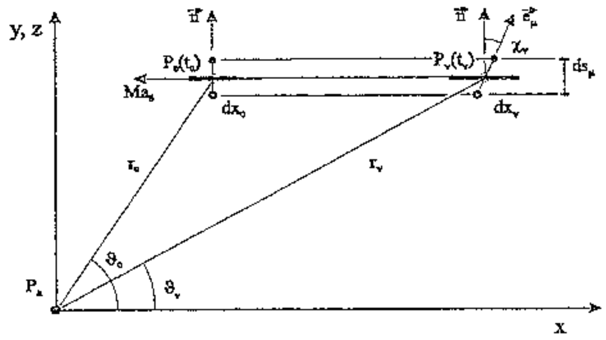

Figure 8: Tilt of doublet vector

6. Direct Sound Pressure Calculation

Sound pressure calculations in the farfield are given by the BERNOULLI formula for unsteady conditions. With the simplification that the induced velocities $\nabla\Phi$ caused by blade and wake do not contribute to the sound pressure in the far field we obtain for the total pressure:

$$p = p_0 - \rho_0 \cdot \frac{\partial \Phi}{\partial t} \qquad (10)$$

or the sound pressure p_S:

$$p_S = \rho_0 \cdot \frac{\partial \Phi}{\partial t} \qquad (11)$$

Now we are able to determine the signature of the sound pressure by calculation of the induced potential, which is radiated from retarded blade and wake surface positions. To obtain the induced potential in the far field of blade and wake panels, it is sufficient to use the far–field versions of the elements in formula (7) instead of lengthy integrations. Time derivatives of the induced potential at the observer point are possible through simple central or backward differences.

7. Results and Comparison

A noise intensive windtunnel testcase of the 'HELISHAPE' project [15] was calculated by the described aerodynamic rotor code, together with a follow–on sound signature determination by the retarded potential postprocessor. Flight condition is 6° descent path with strong BVI effects as already demonstrated in Fig. 1. The result is shown in Figure 9 where the investigated microphone position MIC3 is located 2.3 meter below the rotor disk as indicated in the figure. To retain the visibility, only the free wake of blade 2 is outlined.

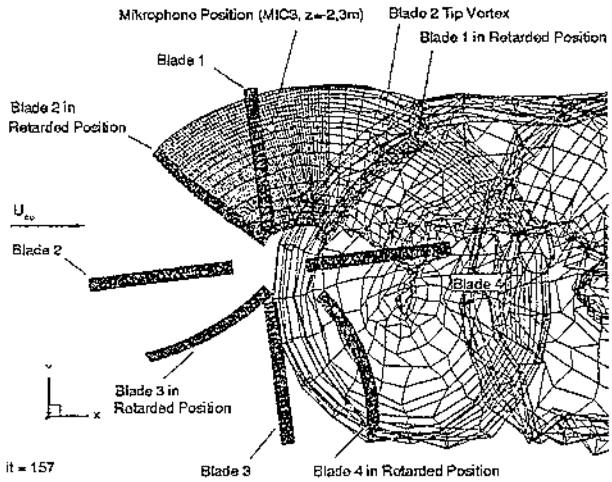

Figure 9: Retarded Rotor Position at Timestep it = 157

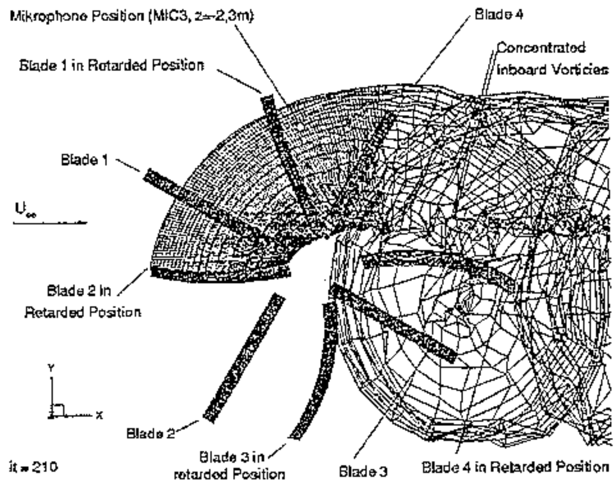

Figure 10: Retarded Rotor Position at Timestep it = 210

Figure 9 illustrates the actual rotor position and the retarded rotor position at timestep number $it = 157$. The retarded rotor is given in relation to the observer at the microphone. All the wake lattice structures between the real and the retarded rotorblades are not yet known or felt at the observer's location. It is visualized here that the retarded rotorblade 1 aligns with its curved shape along the tip vortex of blade 2. This indicates a strong sound pressure signal. We have to expect that the emitted BVI sound of every spanwise rotorblade location arrives at the microphone position simultaneously.

The calculated sound pressure contribution of each blade is given in Figures 11 to 14. From timestep $it = 150$ to $it = 240$ the 4–bladed rotor performs a quarter of rotation. Around $it = 157$ Blade 1 (Fig. 11) generates a very BVI–typical sound pressure line, which was already expected by the visualisation of the retarded blade at the same timestep in Figure 9. Blades 2 and 3 seem to be 'quiet' contributors during this quarter of revolution. More activity is sent by Blade 4 around timestep $it = 210$ while it is in contact with vortices in the rearward rotor disk area (Fig. 10). Figure 15 shows the completely calculated pressure signal of all four blades as a superposition of the single contributions. The curve of 1/4 rotor rotation is now multiplied to a complete rotation of the 4–bladed rotor within a fictive timestep range $it = 150$ to $it = 510$ in Figure 16.

The measured sound pressure signal of a complete rotor rotation in Figure 18 fits well in amplitude but not so well in shape. If the contribution of blade 4 is not taken into account, we receive a shape of the line in Figure 17 which fits very well to the measured signal. In this case the distance between observer (microphone) and the rotor disk was reduced to 1.2 m. The test of the removal of the Blade 4 influence supports the following explanation: Around timestep $it = 210$ where the Blade 4 contribution is strong, the retarded rotorblade passes the area of the rotorshaft wake (Fig. 10). The flow separation behind the rotorshaft is not modeled in the aerodynamic calculation process. Therefore it is realistic to say that the calculated sound pressure signal around the $0°$ rotor position provides too strong and sharp vortex interactions, together with an overprediction of the sound pressure. Further important remarks about the sound pressure prediction are:

- The method is sensitive towards rotor control angles and local changes of the angle of attack. Especially the necessary windtunnel correction which deals with the inclination of the rotor tip path plane must be done carefully.
- The calculations were performed without any friction losses or friction damping such as vortex ageing in the flow field. Vortices keep their strength without any dissipation. There is only a fixed radius for velocity damping around each vortex filament, to ensure aerodynamic code stability.
- Probable dynamic deformations of the rotorblades are not accounted for. The blade flapping was measured during the wind tunnel test and was taken as an input for the calculation.

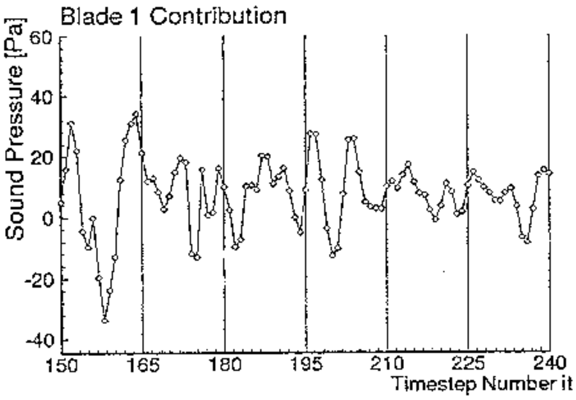

Figure 11: Blade 1 Sound Pressure Contribution

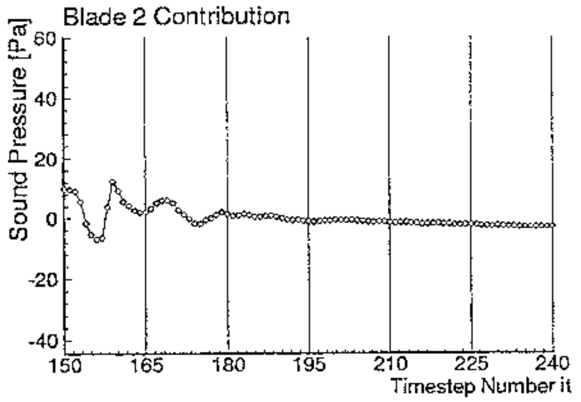

Figure 12: Blade 2 Sound Pressure Contribution

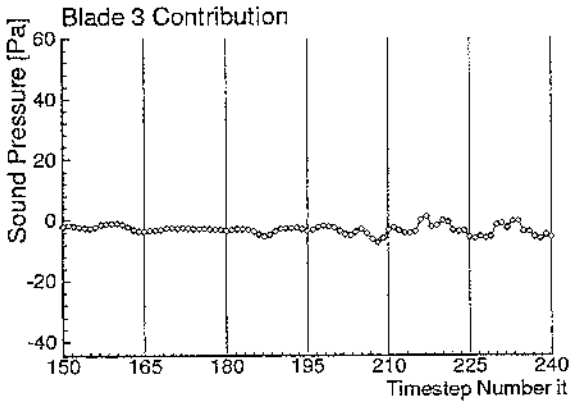

Figure 13: Blade 3 Sound Pressure Contribution

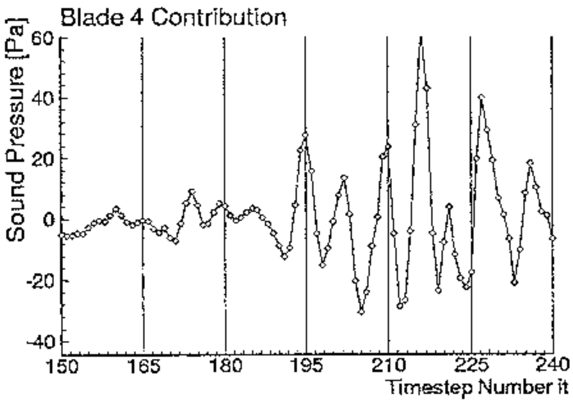

Figure 14: Blade 4 Sound Pressure Contribution

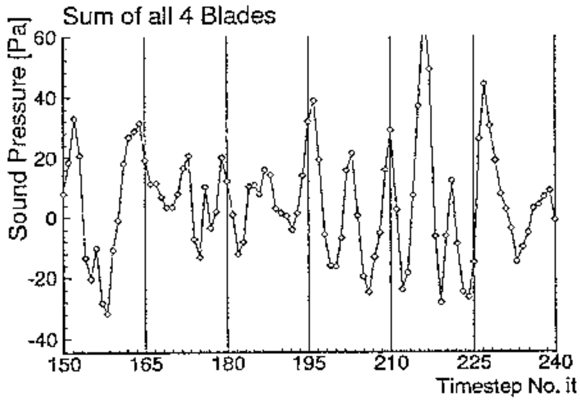

Figure 15: Complete Sum of calculated Sound Pressure at MIC3

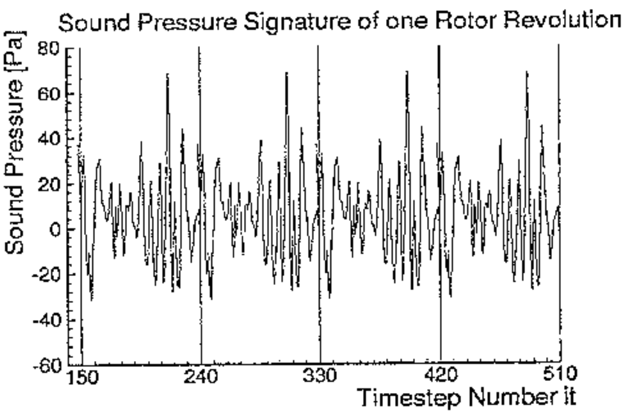

Figure 16: Calculated Sound Pressure of one Rotor Revolution

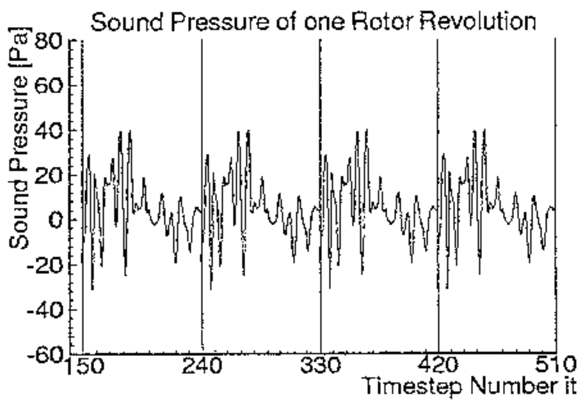

Figure 17: Calculated Sound Pressure, 'Blade 4' Influence Excluded

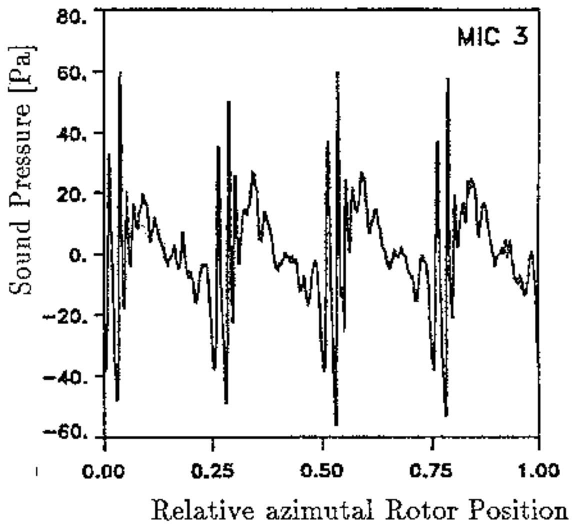

Figure 18: Measured Sound Pressure Signature at MIC 3, x=0,0 m, from HELISHAPE Project

8. Conclusions

The reason to use panel methods to investigate design studies at low computer costs still exists. Extensive aerodynamic rotor wake calculation, 240 timesteps with full time stepping free wake as done in the example presented here, needed about 9 hours CPU at a SGI Impact 10000 workstation (desktop!! machine from the year 1996). The computer time required for the retarded potential postprocessor takes only a few minutes for one observer position. One goal of the whole development done here is to obtain a relatively fast tool for aerodynamic and acoustic investigations at tolerable computer costs. This presentation is to show the capabilities of the 'retarded potential' idea in conjunction with free wake vortex lattice calculations.

The benefit of the direct method is the usage of the induced potential, which is caused by sources and doublets at blade and wake surfaces. Their source and doublet strength is already calculated by the aerodynamic code. It is not necessary to go via induced velocities and blade surface pressure behaviour to gain sound pressure.

Another important point is the unique capability of influence subdivision or influence decomposition. It allows a detailed study of the sound pressure contribution of different rotordisk areas, contributions of single blades or even blade sections. An additional powerful tool is the ability to visualize the retarded rotor position in conjunction with the rotor wake lattice system. Every timestep of interest can be selected and is open for graphical investigation.

With the knowledge of the current development status it will be possible to achieve considerable code speed–up by simplifications and neglection of minor sound pressure contributors. Additional accelerations are possible and already investigated in the field of the aerodynamic code. One point is the rapid rotor free wake calculation by a thin paneled blade with a code internal cross over to a thick panel blade at later timesteps.

If we look further at higher blade tip speeds compressible and transonic effects will increase. An aerodynamic field panel method was already successfully applied to rotors [14] to handle that. The evaluation of the field source activity by the retarded potential method should be possible and could open the way to include high speed impulsive (HSI) noise calculations, too.

References

[1] A. Das. *A unified Approach for the Aerodynamics and Aeroacoustics of Propellers in Forward Motion.* In *AGARD-CP-366 Aerodynamics and Acoustics of Propellers*, Toronto, Canada, October 1984.

[2] A. Das. *Wave Propagation from Moving Singularities and a Unified Exposition of the Linearized Theory for Aerodynamics and Acoustics.* Forschungsbericht DFVLR-FB 84-17, DFVLR, Institut für Entwurfsaerodynamik, Braunschweig, 1984.

[3] F. Farassat. *Introduction to Generalized Functions With Applications in Aerodynamics and Aeroacoustics.* Technical Paper 3428, NASA Langley Research Center, Hampton, Virgina, 1996.

[4] F. Farassat. *The Kirchhoff Formulas for Moving Surfaces in Aeroacoustics – The Subsonic and Supersonic Cases.* Technical Memorandum TM 110285, NASA Langley Research Center, Hampton, Virgina, 1996.

[5] J. E. Ffowcs Williams and Hawkings D. L. *Sound Generation by Turbulence and Surfaces in Arbitrary Motion. Transactions of the Royal Society of London*, Series A, Volume 264:321–342, May 1968.

[6] M. Gennaretti, U. Iemma, and L. Morino. *A Boundary Integral Method for United Transonic Aerodynamics and Aeroacoustic Analysis of Hovering Rotors.* In *AGARD CP–552*, October 1994.

[7] J. Katz and A. Plotkin. *Low-Speed Aerodynamics.* McGraw-Hill Inc., 1991.

[8] G. Kirchhoff. *Zur Theorie der Lichtstrahlen.* In *Annalen der Physik und Chemie, Nummer 18*, pages 663–695. Verlag von Johann Ambrosius Barth, 1883.

[9] M. V. Lowson. *Focusing of Helicopter BVI Noise. Journal of Sound and Vibration*, Vol. 190(3):477–494, 1996.

[10] L. Morino and K. Tseng. *A General Theory of Unsteady Compressible Potential Flows with Applications to Aeroplanes and Rotors* . In P. K. Banerjee and L. Morino, editors, *Boundary Element Methods in Nonlinear Fluid dynamics – Developments in Boundary Element Methods, Volume 6*, pages 183–245. Elsevier Science Publishers Ltd, 1990.

[11] P. M. Morse and H. Feshbach. *Methods of Theoretical Physics.* International Series in Pure and Applied Physics, Vol. I. McGraw–Hill Book Company, Inc., 1953.

[12] L. Prandtl. *Theorie des Flugzeugtragflügels im zusammendrückbaren Medium . Luftfahrtforschung*, 13(10):313–319, Oktober 1936.

[13] A. Röttgermann, R. Behr, Ch. Schöttl, and S. Wagner. *Calculation of Blade–Vortex Interaction of Rotary Wings in Incompressible Flow by an Unsteady Vortex–Lattice Including Free Wake Analysis.* In W. Hackbusch, editor, *Numerical Technics for Boundary Element Methods*, volume 33 of *Notes on Numerical Fluid Mechanics*, pages 153 – 166. Vieweg Verlag, 1991.

[14] A. Röttgermann and S. Wagner. *Cost Efficient Calculation of Compressible Potential Flow Around a Helicopter Rotor Including Free Vortex Sheet by a Field Panel Method.* In *AGARD CP–552*, October 1994.

[15] K. J. Schultz, W. Splettstösser, B. Junker, W. Wagner, E. Schöll, G. Arnaud, E. Mercker, K. Pengel, and D. Fertis. *A Parametric Wind Tunnel Test on Rotorcraft Aerodynamics and Aeroacoustics (HELISHAPE) – Test Procedures and Representative Results.* In *Proceedings of the 22. European Rotorcraft Forum*, Brighton, UK, September 1996. Paper No. 52.

[16] D. Wehr, L. Zerle, and S. Wagner. *Coupling Euler and Potential Methods for Rotors in Unsteady Forward Flight.* In *Proceedings of the 22. European Rotorcraft Forum*, Brighton, UK, September 1996. Paper No. 59.

[17] L. Zerle and S. Wagner. *Development and Validation of a Vortex Lattice Method to Calculate the Flowfield of a Helicopter Rotor Including Free Wake Development.* In *Proceedings of the 18. European Rotorcraft Forum*, Avignon, France, September 1992. Paper No. 72.

[18] L. Zerle and S. Wagner. *Influence of Inboard Shedded Rotor Blade Wake to the Rotor Flow Field.* In *Proceedings of the 19. European Rotorcraft Forum*, Como, Italy, September 1993. Paper No. C13.